# RNA Unwinding Activity of the Hepatitis C Virus NS3 Helicase Is Modulated by the NS5B Polymerase†

Thomas A. Jennings,‡ Yingfeng Chen,‡ Deniz Sikora,‡ Melody K. Harrison,‡ Bartek Sikora,‡ Luyun Huang,‖ Eckhard Jankowsky,§ Margaret E. Fairman,§ Craig E. Cameron,‖ and Kevin D. Raney*,‡

*Department of Biochemistry and Molecular Biology, University of Arkansas for Medical Sciences, Little Rock, Arkansas 72205, Department of Biochemistry, Case Western University, Cleveland, Ohio 44106, and Department of Biochemistry and Molecular Biology, The Pennsylvania State University, University Park, Pennsylvania 16802*

*Received May 30, 2007; Revised Manuscript Received November 14, 2007*

ABSTRACT: Hepatitis C virus (HCV) infects over 170 million persons worldwide. It is the leading cause of liver disease in the U.S. and is responsible for most liver transplants. Current treatments for this infectious disease are inadequate; therefore, new therapies must be developed. Several labs have obtained evidence for a protein complex that involves many of the nonstructural (NS) proteins encoded by the virus. NS3, NS4A, NS4B, NS5A, and NS5B appear to interact structurally and functionally. In this study, we investigated the interaction between the helicase, NS3, and the RNA polymerase, NS5B. Pull-down experiments and surface plasmon resonance data indicate a direct interaction between NS3 and NS5B that is primarily mediated through the protease domain of NS3. This interaction reduces the basal ATPase activity of NS3. However, NS5B stimulates product formation in RNA unwinding experiments under conditions of excess nucleic acid substrate. When the concentrations of NS3 and NS5B are in excess of nucleic acid substrate, NS5B reduces the rate of NS3-catalyzed unwinding. Under pre-steady-state conditions, in which NS3 and substrate concentrations are similar, product formation increased in the presence of NS5B. The increase was consistent with 1:1 complex formed between the two proteins. A fluorescently labeled form of NS3 was used to investigate this interaction through fluorescence polarization binding assays. Results from this assay support interactions that include a 1:1 complex formed between NS3 and NS5B. The modulation of NS3 by NS5B suggests that these proteins may function together during replication of the HCV genome.

The hepatitis C virus (HCV[1]) has caused a global crisis by infecting more than 2% of the world's population (*1*). Combination therapies using interferon and the antiviral drug ribavirin are effective in only some patients, and such treatments are costly and cause debilitating side effects (*2*, *3*). Vaccine and drug development has been difficult because the only natural hosts for HCV are humans and chimpanzees, and only recently has the virus been cultivated *in vitro* (*4*−*6*). As a result, the enzymes encoded by the virus have been intensely studied for rational drug design. HCV encodes an RNA-dependent RNA polymerase, NS5B, which is required for viral replication. A multifunctional protein, NS3, is also encoded which contains ATPase, helicase, and protease activities. Several groups have reported potent compounds that inhibit the HCV NS5B RNA polymerase and the HCV NS3 serine protease (*7*, *8*). However, few inhibitors of the HCV helicase have been explored as antivirals because less is known about the mechanism of action of the HCV helicase and possibly because of the lack of substrate specificity exhibited by helicases (*9*).

HCV NS3 helicase is a 3′-to-5′ helicase (*10*). The N-terminal 180 amino acids of the NS3 protein manifest protease activity and the C-terminal 450 amino acids are responsible for NTPase and helicase activity. Its crystal structure has been solved (*11*, *12*), leading to the suggestion of an inchworm mechanism for nucleic acid unwinding. More recently, a Brownian motor mechanism has been proposed for NS3 helicase unwinding (*13*). HCV NS5B is an RNA-dependent RNA polymerase. NS5B is able to synthesize RNA by using various RNAs as templates. Its crystal structure has also been solved and indicates the 'right-hand' convention as described for other polymerases (*14*).

Replication of HCV RNA occurs in a membrane-bound replication complex containing nonstructural proteins (*15*). Two of the these proteins, NS4A and NS4B, may recruit the complex to the membrane (*16*, *17*). Several labs have obtained evidence for a protein complex that involves many of the nonstructural (NS) proteins encoded by the virus (*18*−*24*). NS3, NS4A, NS4B, NS5A, and NS5B appear to interact with each other based on co-immunoprecipitation (*18*, *21*), far-western blotting (*22*), and enzymatic assays (*22*−*24*). Studying the protein−protein interaction in the replication

† This work was supported by NIH R01 grant AI060563 (K.D.R. and C.E.C.) and GM067700 (E.J.), by NIH INBRE grant P20 RR016460, and by funds from the UAMS Graduate Student Research Fund (T.A.J.).

* Author to whom correspondence should be addressed: Tel.: (501) 686-5244, fax: (501) 686-8169, e-mail: raneykevind@uams.edu.

‡ University of Arkansas for Medical Sciences.

§ Case Western University.

‖ The Pennsylvania State University.

[1] Abbreviations: HCV, hepatitis C virus; NS, nonstructural protein; NPH-II, nucleoside triphosphate phosphohydrolase II; SPR, surface plasmon resonance.

10.1021/bi701048a CCC: $40.75 
Published on Web 01/08/2008

complex therefore appears important for understanding the assembly of the HCV replication complex and the mechanism and regulation of individual NS proteins during RNA synthesis.

Several groups have reported interactions between DNA polymerases and DNA helicases. Von Hippel and co-workers (*25*) studied the molecular mechanism of the functional coupling of the helicase (gp41) and polymerase (gp43) of bacteriophage T4 within the DNA replication fork. They reported that the unwinding rate of gp41 was significantly increased by the trailing of gp43 although physically these two proteins might not interact with each other. The T7 gene 4 helicase was found to interact with the T7 DNA polymerase nearly three decades ago (*26*, *27*), and this system continues to be of interest in studying helicase-polymerase interactions (*28*, *29*). Recently, the Patel group reported that T7 DNA polymerase may increase the unwinding rate of T7 DNA helicase by 'pushing' the helicase or by preventing the helicase from 'slipping' (*29*). The Ahlquist group has investigated the interaction between a viral RNA polymerase and a helicase-like protein in the Brome mosaic virus. They reported that the 1a helicase-like protein and 2a polymerase-like protein can colocalize in vivo in an endoplasmic reticulum-associated replication complex that is the site of BMV-specific RNA synthesis. The helicase-like protein 1a controls or contributes to template specificity in RNA replication (*30*). All these studies point to the important functional interaction between helicase and polymerase for both DNA and RNA viral replication.

Previously, Zhang, et al. have demonstrated that the interaction between NS3 and NS5B results in an increase of product formation under steady-state conditions (*23*). In the present study, we detected a direct interaction between NS3 and NS5B by affinity pull-down, surface plasmon resonance, and fluorescence polarization. We have also examined, for the first time, the effect of NS5B on NS3-catalyzed RNA unwinding. We extend the work of Zhang et al. by investigating the functional interaction between NS3 and NS5B on NS3-catalyzed unwinding under steady state, single turnover, and pre-steady-state conditions. We find that NS5B can significantly enhance NS3-catalyzed product formation for unwinding RNA and DNA under steady-state conditions, in which the nucleic acid is in excess of the enzyme concentration and multiple enzymatic turnovers are allowed. In contrast, under single turnover conditions, where the concentrations of NS3 and NS5B greatly exceed substrate concentration and dissociated enzyme is prevented from rebinding to substrate, NS5B reduces NS3-catalyzed RNA and DNA unwinding activity. Analysis by pre-steady-state conditions, in which enzyme and substrate concentrations are similar and multiple turnovers allowed, we find that the unwinding rate of NS3 is not enhanced by the addition of NS5B. The increase in product formation is most likely due to enhanced association. We also observed that NS5B does not interact strongly with NS3 helicase domain, indicating that the protease domain primarily mediates the interaction, as observed by others (*21*, *23*).

## MATERIALS AND METHODS

*Materials.* 4-(2-Hydroxyethyl)-1-piperazineethanesulfonic acid (HEPES), ethylenediamine tetracetic acid (EDTA), $\beta$-mercaptoethanol (BME), sodium dodecyl sulfate (SDS), 3-(*N*-morpholino)propanesulfonic acid (MOPS), 2-amino-2-hydroxymethyl-1,3-propanediol (Tris), NaCl, acrylamide, bisacrylamide, $MgCl_2$, KOH, ATP, formamide, xylene cyanole, bromophenol blue, urea, and glycerol were purchased from Fisher. Nitrilotriacetate sensor chips were purchased from Biacore. Sephadex G-25, BSA (bovine serum albumin), pyruvate kinase/lactate dehydrogenase (PK/LDH), nicotinamide adenine dinucleotide (NADH), ATP, and phosphoenolpyruvate (PEP) were from Sigma. Poly U was purchased from Amersham Pharmacia Biotech. DNA oligonucleotides were from Integrated DNA Technologies and purified by preparative gel electrophoresis (*31*). [$\gamma$-32P]ATP was purchased from Perkin-Elmer Life Sciences. T4 polynucleotide kinase was obtained from New England Biolabs. Recombinant full-length NS3 was cloned from Con1b, and NS5B$\Delta$C21-C-$his_6$ (referred to as NS5B throughout the text), was derived from 1b strain BK. Proteins were expressed and purified as previously described (*32*, *33*). NS3h was expressed as a truncation containing the C-terminal 465 amino acids and purified in a fashion analogous to full length NS3 (*32*). NPH-II was kindly provided by Dr. Eckhard Jankowsky.

*Conjugation of NS5B to Dynabead*s. Two sets of Dynabeads (Invitrogen) were prepared. To produce NS5B-coated beads, 0.3 mg of purified NS5B (which had been dialyzed into PBS, pH 7.4) was coupled to 5 mg of epoxy-activated Dynabeads (M-270) according to manufacturer's protocols. To produce control beads, an identical volume of PBS alone was added to 5 mg of epoxy-activated Dynabeads and quenched with glycine.

*Dynabead Pull-Down Assay.* A 0.83 mg amount of NS5B-conjugated or quenched beads were added to 2.5 $\mu$M purified NS3 or NS3h in a total volume of 300 $\mu$L. The incubation buffer was 25 mM HEPES, pH 7.5, 1 mM $\beta$-mercaptoethanol, 0.1 mM EDTA, 0.1% Tween-20, and either 175, 225, or 300 mM NaCl. The beads and protein were incubated at 4 °C for 1 h with gentle mixing. The beads were then washed five times with buffer identical to the respective incubation conditions. Washed beads were suspended in SDS-PAGE sample buffer and boiled for 10 min to elute interacting proteins. Eluted proteins were resolved by SDS-PAGE and visualized by staining with SYPRO Ruby protein gel stain. Pull-down assay with NS3-tetracys and NS3-FlAsH was performed similarly using 2 mg of NS5B-conjugated Dynabeads, 5 $\mu$M protein, and incubation buffer containing 25 mM HEPES, pH 7.5, 250 mM NaCl, 0.1 mM EDTA, and 0.1% Tween-20. The beads were washed five times and then boiled in nonreducing SDS-PAGE sample buffer. Eluted proteins were resolved by SDS-PAGE and visualized both by Coomassie staining and by fluorescent imaging on a Molecular Dynamics Storm 840 imaging system.

*FlAsH Labeling of NS3.* A form of NS3 was engineered to have a tetracysteine cassette (cys−cys-pro-gly-cys-cys) located at the C-terminus of the protein. The protein and FlAsH-$EDT_2$ (Invitrogen) were incubated at 4 °C for 5 h with gentle agitation. After dialysis to remove free dye, approximately 85% of the protein was found to have bound the dye. The resulting labeled protein was referred to NS3-FlAsH.

*Fluorescence Polarization with NS3-FlAsH and NS5B.* Measurements were made at 37 °C using a Perkin-Elmer

Victor$^3$V 1420 Multilabel Counter. Measurements were integrated over a 0.2 s detection period. The instrument lamp energy was at the maximum setting, and filters were set to 485 nm for excitation and 535 nm for emission. The polarizing aperture was set to normal, and the excitation aperture was set to 4 mm. NS3-FlAsH at 50, 100, or 150 nM was titrated against an increasing concentration of NS5B in buffer containing 25 mM HEPES, pH 7.5, and 50 mM NaCl. Triplicate samples were incubated at 37 °C for 90 min prior to measuring fluorescence polarization. Data were plotted as the average of three independent experiments with standard deviations.

*Fluorescence Polarization with Fluorescein-Labeled DNA.* DNA substrate (5′-fluorescein labeled DNA, F-$(T)_{15}$) was purchased from Integrated DNA Technologies and purified by preparative gel electrophoresis. The fluorescence polarization buffer consisted of 50 mM MOPS-$K^+$ (pH 7.0), 50 $\mu$M EDTA, 0.1 mg/mL BSA, and 10 mM NaCl. Varying concentrations of NS5B were incubated with 0.1 nM F-$(T)_{15}$ DNA in fluorescence polarization buffer for 3 min at 37 °C in a final volume of 1 mL per sample. Fluorescence polarization was monitored on a Beacon Fluorescence Polarization Instrument (PanVera). Fluorescence polarization buffer was used as the blank. The change in millipolarization (mP) units was determined using a sample of 0.1 nM fluorescein-labeled DNA as the zero point. Fluorescence polarization data were fit to a quadratic equation to obtain $K_D$ values (KaleidaGraph software). The following equation was used:

$$mP = \frac{\dfrac{\Delta mP}{[\mathrm{DNA}]} \times (K_D + [\mathrm{DNA}]_T + [\mathrm{E}]_T) - \sqrt{(K_D + [\mathrm{DNA}]_T + [\mathrm{E}]_T)^2 - 4[\mathrm{E}]_T[\mathrm{DNA}]_T}}{2[\mathrm{DNA}]_T}$$

where ΔmP is the total change in millipolarization, [DNA] is the concentration of fluorescently labeled DNA, [E] is the concentration of NS5B, and $K_D$ is the apparent equilibrium dissociation constant.

*Surface Plasmon Resonance*. A BIAcore 3000 instrument (BIAcore AB) for real-time monitoring of interaction between proteins was used for investigation of interactions between NS5B and NS3. The nitrilotriacetate sensor chip flow channel was first saturated with nickel by passing 20 $\mu$L of a 500 mM $NiCl_2$ solution at a flow rate of 20 $\mu$L/min. Then purified his-tagged NS5B was immobilized to flow channel 2 only at concentrations of 500 nM in HBS-EP (BIAcore AB) running buffer pH8.0 at a flow rate of 20 $\mu$L/min. Flow channel 1 of the sensor chip was mocked with nickel as a nonspecific binding control. The binding experiment was performed at room temperature with HBS-EP (BIAcore AB) as running buffer. A 500 nM solution of NS3 or NS3 helicase domain was injected into both flow channels at a flow rate of 20 mL/min. The binding of NS3 or NS3 helicase domain to immobilized NS5B was measured as a change in resonance signal. Dissociation was recorded over 7 min. Nonspecific binding of NS3 or NS3 helicase domain with the surface was subtracted from each measurement. Regeneration of the flow cells was performed by passing 20 mL of 350 mM EDTA in eluent buffer at 20 mL/min. Sensorgrams were analyzed with BIAevaluation 3.0 (BIAcore).

*ATPase Assays*. NS3 ATPase activities were monitored spectrophotometrically with the assay described previously (*34*). All assays were performed at 37 °C in buffer containing 25 mM MOPS, pH 7.0, 10 mM NaCl, 10 mM $MgCl_2$, 5 mM ATP, 50 $\mu$M EDTA, 10 units/mL phosphoenolpyruvate kinase/lactate dehydrogenase (PK/LDH), 4 mM phosphenolpyruvate (PEP), 0.7 mg/mL NADH, and 0.1 mg/mL bovine serum albumin (BSA). The concentration of NS3 was 100 nM. After measurement of the basic activity of NS3, 100 nM NS5B was added and the ATPase activity was measured. Following this, various concentrations of poly U were introduced and the activity was detected. The concentration of poly U is indicated in the figure legend. The assay time is 30 s. Observed ATP hydrolysis rates were obtained by measuring the conversion of NADH to $NAD^+$ at 380 nm with an extinction coefficient of 1210 $M^{-1}$ $cm^{-1}$. The oxidation of 1 mol of NADH corresponds to the hydrolysis of 1 mol of ATP. The specific activity was calculated by observed ATP hydrolysis rate divided by enzyme concentration.

*Unwinding Assays*. The nucleic acid substrates for unwinding studies are referred to as 60:30mer and 45:30mer. The substrates contain either 30 nt or 15 nt of single-stranded nucleic acid overhang on the loading strand, respectively, and 30 base pairs of dsNA. The sequence of the RNA 60mer loading strand was 5′-GACTGACGCTAGGCTGACAG-GACGTACTAC$U_{30}$-3′. The sequence of the 30mer complementary strand was 5′-GTAGTACGTCCTGTCAGC-CTAGCGTCAGTC-3′. For DNA unwinding experiments, the sequence was the same except for the replacement of uridine with thymidine. Substrates were purified and radiolabeled as described (*31*). Unwinding experiments were performed with a water bath maintained at 37 °C. All concentrations listed are after mixing. Unwinding buffer consisted of 25 mM MOPS-$K^+$ (pH 7.0), 50 $\mu$M EDTA, 0.1 mg/mL BSA, and 10 mM NaCl. The RNA or DNA 60:30mer was incubated with NS3 and/or NS5B prior to initiating the unwinding reaction with 5 mM ATP and 5 mM $MgCl_2$. To prevent reannealing of ssNA products, a 30-fold excess of 30mer that was complementary to the 30mer in the 60:30mer or 45:30mer was added along with the ATP. Assays performed under single turnover conditions contained 75 $\mu$M poly U protein trap in the ATP−$MgCl_2$−30mer solution to prevent protein from being able to rebind 60:30mer substrate after dissociation (*35*). After rapid mixing of the NS3-nucleic acid substrate solution with the ATP−$MgCl_2$−30mer solution, the reaction was quenched with 200 mM EDTA plus 0.7% SDS. A 10 $\mu$L aliquot of the quenched unwinding reaction was added to 5 $\mu$L of 6X loading buffer (30% glycerol, 0.1% bromophenol blue, 0.1% xylene cyanole), and analyzed on a 20% polyacrylamide gel. The amount of free 60mer and 60:30mer or free 45mer and 45:30mer was quantified with a Molecular Dynamics Phosphorimager and ImageQuant software (*32*, *36*).

## RESULTS

*NS5B-Coated Dynabead Pull-Down Assays.* Several groups have used different approaches to indirectly assess the interaction between NS3 and NS5B. Interaction between NS3 and NS5B has been identified by co-immunoprecipitation analysis, yeast two-hybrid assay, and a far-western blot assay (*18*, *21*, *22*). To directly observe the interaction between NS3

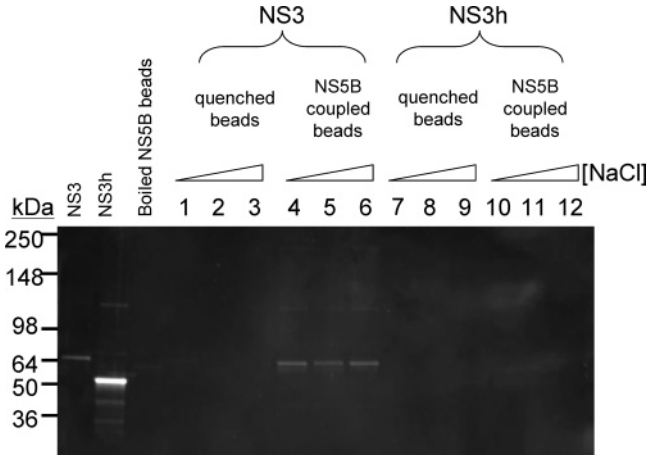


FIGURE 1: NS5B-coated Dynabead pull-down assay. NS5B-coated beads were incubated with NS3 or NS3h at three different salt concentrations: 175, 225, and 300 mM NaCl as indicated by the ramps. As a control, glycine quenched beads were also included. Products from the pull-down were resolved by 4−20% SDS-PAGE and visualized by SYPRO Ruby staining. Recombinant NS3 and NS3h were run in separate lanes for reference.

and NS5B, NS5B-coated Dynabeads were used to isolate recombinant NS3 from solution. NS5B was covalently linked to epoxy-coated Dynabeads, followed by washing to remove excess protein. NS5B-coated Dynabeads were incubated with NS3 for 1 h, followed by washing to remove unbound protein. To test the stringency of the interaction, three different salt concentrations were used in the washing step. As demonstrated by the products isolated from the pull-down assay, NS3 binds equally well under the three different salt concentrations, indicating that the interaction is not highly dependent on electrostatic interactions (lanes 4−6, Figure 1). A similar experiment was performed in which NS3 helicase domain (NS3h) was incubated with the NS5B-coated Dynabeads. No protein was isolated from these pull-down experiments, indicating that the protease domain of NS3 is likely involved in the interaction between NS3 and NS5B (lanes 10−12, Figure 1). This observation is in good agreement with previously described findings (*21*, *23*). Additional controls for nonspecificity included incubating Dynabeads that had been quenched with glycine with NS3 and NS3h, separately. A trace amount of NS3 was found to bind nonspecifically to the quenched Dynabeads under the 175 mM salt condition (lane 1, Figure 1). However, increasing the salt concentration eliminated nonspecific binding. NS3 helicase domain was not found to bind to the quenched Dynabeads under any conditions.

*Interaction between NS5B and NS3 by Surface Plasmon Resonance (SPR).* To further study the interaction between NS3 and NS5B, surface plasmon resonance was we applied surface plasmon resonance. A BIAcore sensor chip designed for docking $(his)_6$-tagged protein was utilized to immobilize purified, $(his)_6$-tagged NS5B on the surface of the chip (Figure 2). The binding phase revealed a rapid binding event followed by slower binding to the chip. NS3 was injected, resulting in a strong resonance difference that indicated a direct interaction between NS5B and NS3. Quantitative analysis of the BIAcore data was not pursued because NS5B and NS3 exist as oligomers in solution (*37*−*39*), which greatly complicates quantitative evaluation of SPR data. A similar experiment was performed by injecting NS3h to

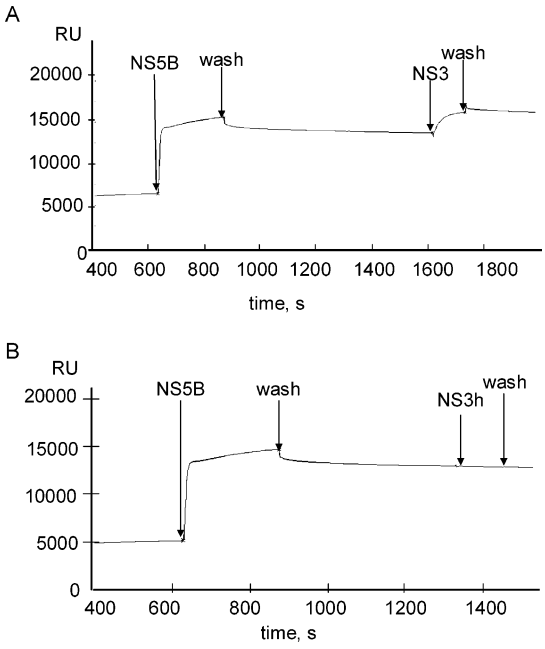


FIGURE 2: Interaction between NS5B and NS3 by surface plasmon resonance (SPR). (A) $(His)_6$-NS5B (500 nM) was injected onto one activated NTA sensor chip flow channel (from position "NS5B" to "wash"), resulting in about 8000 response units (RU). The NS5B-bound chip was washed with buffer to remove excess NS5B. NS3 (500 nM) was injected onto the NS5B channel and the control channel (from position "NS3" to "wash") resulting in an increase response of about 2490 RU (subtraction from the two channels). (B) $(His)_6$-NS5B (500 nM) was injected onto one NTA sensor chip flow channel (from position "NS5B" to "wash"), resulting in about 8000 response units (RU). The NS5B-bound chip was washed with buffer to remove excess NS5B. NS3 helicase domain (500 nM) was injected onto the NS5B channel and the control channel (from position "NS3h" to "wash"). No response difference was detected.

determine whether it also binds to NS5B; however, no resonance difference was observed (Figure 2B). Taken together with the pull-down assay, the data demonstrate that the interaction between NS3 and NS5B may involve the NS3 protease domain. This finding is in good agreement with published results showing that the direct interaction between NS3 and NS5B required the N-terminal region of NS3 (*21*). The initial, multiphase binding event may be due to rapid association of NS5B to the $Ni^{+2}$-coated surface, followed by additional binding due to the oligomeric nature of NS5B. Chemical cross-linking (Supporting Information Figure 1) and size-exclusion chromatography (Supporting Information Figure 2) indicate that NS5B exists as an oligomer at pH 7.0, which is optimal for NS3-catalyzed RNA and DNA unwinding activity.

*NS5B Inhibits NS3 Basal and Poly U Stimulated ATPase Activity.* Prior reports showed the activity of HCV NS5B was stimulated by NS3 (*22*), and that NS5B interaction with NS3 stimulates NS3-catalyzed DNA unwinding activity (*23*). However, the primary biological substrate for NS3 is RNA, and significant differences exist when comparing NS3 activity on DNA compared to RNA. For example, NS3-catalyzed RNA unwinding is much more sensitive to pH than DNA unwinding (*40*). Additionally, the existing data did not evaluate helicase activity under varying protein concentrations. We first analyzed the basal and poly U-stimulated ATPase activity of NS3 in the absence and presence of NS5B. Surprisingly NS5B decreased NS3 basal ATPase

activity (Figure 3A). The inhibition of NS3 ATPase activity by NS5B was completely overcome by addition of excess poly U (Figure 3A). Figure 3B shows that the poly U stimulated ATPase activity was reduced by adding excess NS5B. The effect of NS5B on NS3's poly U-stimulated ATPase activity was further investigated by varying poly U in the presence or absence of NS5B. The concentration of poly U needed to reach maximal ATPase activity was increased when NS5B was present (Figure 3C). For example, when 200 nM NS5B was present in the solution (open triangles, Figure 3C), more than 5 $\mu$M poly U was needed to stimulate the ATPase activity. This result is consistent with that seen in Figure 3B, and is likely due to NS5B completing for binding of poly U.

*NS5B Increases the Activity of NS3-Catalyzed Unwinding of an RNA Substrate When Nucleic Acid Substrate Concentration Is Equal to NS3 Concentration.* To determine whether the interaction between NS3 and NS5B affected RNA unwinding activity, we used an RNA substrate with a long single-stranded overhang (30 nt) in order to accommodate binding of both NS3 and NS5B. NS3 requires a single strand overhang for efficient unwinding and each NS3 molecule can bind ~8 nucleotides (*41*). NS5B can bind around 8−10 nucleotides (*42*). NS3 was incubated with an equimolar quantity of RNA substrate followed by initiation of the unwinding reaction by addition of ATP and $MgCl_2$. Very little ssRNA product resulted over a 25 min reaction period (Figure 4). When we introduced an equal amount of NS5B into the reaction, around 30% of the substrate was unwound after 25 min. Increasing the amount of NS5B in the reaction led to ~75% of the substrate being unwound over 25 min.

*NS5B Reduces the Ability of NPH-II-Catalyzed Unwinding of an RNA Substrate.* To investigate whether the modulation NS5B exerts on NS3 unwinding is specific for the NS3−NS5B interaction or a generic effect due to the ability of NS5B to bind RNA, the effect of NS5B on another 3′-to-5′ RNA helicase, vaccinia virus nucleoside triphosphate phosphohydrolase II (NPH-II), was studied. NPH-II is also a member of the DExH/D family of proteins, a subset of helicase superfamily 2 (SF2). It has been shown to possess robust and processive RNA helicase activity (*43*). NPH-II (10 nM) was incubated with increasing concentrations of NS5B and the RNA substrate. The reactions were initiated by the addition of ATP under steady-state conditions in which NS5B was found to stimulate the activity of NS3 (see Figure 4). The presence of NS5B was found to reduce NPH-II RNA unwinding in a concentration-dependent manner (Figure 5). NS5B can bind to the RNA substrate and is likely able to compete for binding with NPH-II. These data indicate that the interaction between NS3 and NS5B produces specific enhancement of NS3-catalyzed RNA unwinding activity.

*NS5B Enhances the Ability of NS3-Catalyzed Unwinding of a DNA Substrate When Substrate Concentration Is Equal to NS3 Concentration.* NS3 is a proficient helicase for unwinding DNA substrates as well as RNA substrates (*32*, *44*, *45*). To determine whether the interaction between NS5B and NS3 stimulated the DNA helicase activity of NS3, experiments were conducted with a DNA substrate. NS3 (250 nM) was incubated with the 60:30mer DNA substrate (250 nM) in the presence of increasing amounts of NS5B. Substantially greater product formation is observed in the presence of NS5B (Figure 6). This result further supports

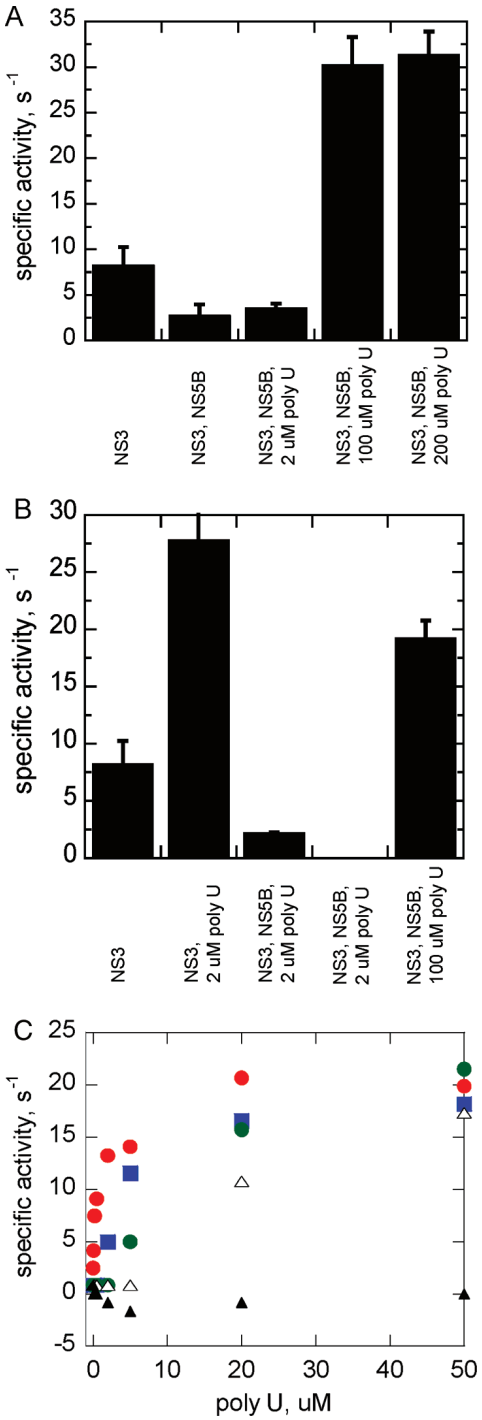


FIGURE 3: The effect of NS5B on the ATPase activity of NS3. ATPase activity was monitored by using a enzyme-coupling system in a spectrophotometric assay. The order of addition of each reagent is described as follows: (A) Column 1, 100 nM NS3; Column 2, 100 nM NS5B was added to the mixture from column 1 resulting in reduced specific activity; Column 3, 2 mM poly U (in nucleotides) was added to the mixture in column 2; Column 4, 100 mM poly U was added to the mixture in column 3; Column 5, 100 mM poly U was added to the mixture in column 4. (B) Column 1, 100 nM NS3; Column 2, 2 mM poly U was added to the mixture in column 1; Column 3, 100 nM NS5B was added to the mixture in column 2; Column 4, 400 nM NS5B was added to the mixture in column 3; Column 5, 100 mM poly U was added to the mixture in column 4. (C) Enzyme concentrations were held constant as increasing poly U was titrated into the mixture: 100 nM NS3 (red circles); 100 nM NS3, 50 nM NS5B (blue squares); 100 nM NS3, 100 nM NS5B (green circles); 100 nM NS3, 200 nM NS5B (open triangles); 200 nM NS5B (closed triangles).

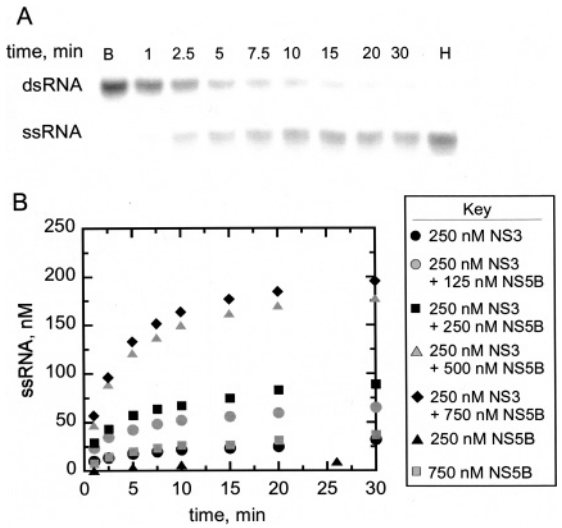


FIGURE 4: NS5B stimulates NS3-catalyzed unwinding of RNA when concentrations of enzyme and substrate are similar. NS3 and NS5B were preincubated 5 min at room temperature before adding 60:30mer RNA substrate. The enzyme−substrate mixture was incubated an additional 5 min at 37 °C followed by initiation of the unwinding reaction by addition of ATP. (A) Phosphorimage of a native gel separating single-stranded RNA from double-stranded RNA. Times of reaction are indicated above each lane, as well as *B* for a blank sample that has not been unwound, and *H* for a heated sample in which all of the substrate has been melted. (B) Unwinding of 250 nM 60:30merRNA with 250 nM NS3 in the absence of NS5B (filled circles), or in the presence of 125 nM NS5B (gray circles), 250 nM NS5B (closed squares), 500 nM NS5B (gray triangles), and 750 nM NS5B (filled diamonds). As controls, there are reactions containing no NS3 with 250 nM NS5B (filled triangles) and 750 nM NS5B (gray squares).

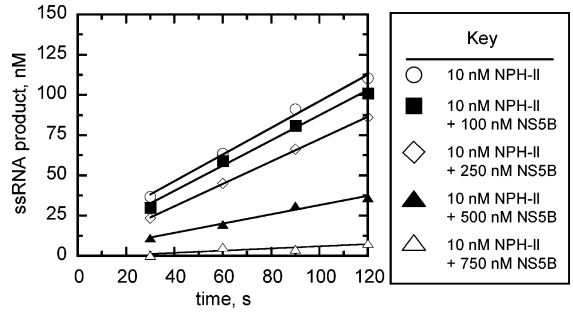


FIGURE 5: NS5B does not enhance the helicase activity of NPH-II. (A) 10 nM NPH-II unwinds 250 nM 60:30mer RNA in the absence (open circles) or presence of 100 nM NS5B (filled squares), 250 nM NS5B (open diamonds), 500 nM NS5B (filled triangles), and 750 nM NS5B (open triangles). NPH-II and NS5B were preincubated 5 min at room temperature before adding 60:30mer RNA substrate. The reactions were initiated by the addition of 3.5 mM ATP and 3.5 mM $MgCl_2$. Reactions were quenched at 30, 60, 90, and 120 s by the addition of 200 mM EDTA/0.7% SDS. Radiolabeled products were resolved by 20% native polyacrylamide gel electrophoresis and visualized by phosphorimager analysis.

the specific enhancement of NS3-catalyzed product formation in the presence of NS5B.

*NS5B Reduces the Ability of NS3-Catalyzed Unwinding under the Single Turnover Condition.* The previous experiments were performed under multiple-cycle conditions. Under these conditions, multiple cycles of DNA or RNA unwinding can occur such that dissociation or association of enzyme with substrate might limit the observed rate of product formation. To examine the steps involved with DNA or RNA more directly, single-turnover experiments were

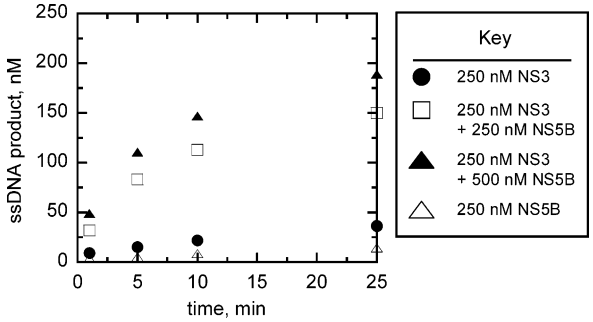


FIGURE 6: NS5B stimulates NS3-catalyzed unwinding of DNA when concentrations of enzyme and substrate are similar. Unwinding of 250 nM 60:30mer DNA with 250 nM NS3 in the absence of NS5B (filled circles) or in the presence of 250 nM NS5B (open squares), 500 nM NS5B (filled triangles). As a control, there is a reaction having 250 nM 60:30mer DNA and 250 nM NS5B but no NS3 (open triangles).

performed in the presence of excess enzyme concentration over substrate concentration. NS3 (300 nM) and 30 or 300 nM NS5B were preincubated before adding 2 nM RNA substrate. The reactions were initiated by adding ATP, $MgCl_2$, and an excess quantity of annealing trap (60 nM) and protein trap (75 $\mu$M poly U). A 300 nM NS3 concentration alone can unwind approximately 40% of the substrate (Figure 7). With the addition of 30 nM NS5B, the observed rate constant for product formation is slower but the amplitude is the same (Figure 7A, Table 1). When NS3 (300 nM) is incubated with an equal amount of NS5B (300 nM), RNA unwinding was reduced to negligible levels. Similar results were found for unwinding of DNA under single turnover conditions (Figure 7B). Hence, NS5B can reduce NS3-catalyzed unwinding under conditions in which the enzyme concentration is in great excess of the substrate concentration. It is possible that NS5B competes for binding to the substrate under conditions where substrate is limiting because NS5B is known to bind tightly to RNA. Likewise, NS5B is capable of binding tightly to ssDNA as exhibited by fluorescence polarization using a 5′-fluorescein-labeled 15mer (Figure 7C). The presence of NS5B leads to formation of nonproductive complexes with RNA or DNA when the concentration of nucleic acid substrate is limiting.

*Fluorescence Polarization with NS3-FlAsH and NS5B.* In order to examine the interaction between NS3 and NS5B in solution, a fluorescently labeled form of NS3 was prepared. A peptide containing four cysteines, cys−cys-pro-gly-cys-cys, was fused to the C-terminus of NS3. NS3-tetracys was found to behave similarly to NS3 in ATPase activity and DNA unwinding (Sikora et al., in preparation). NS3-tetracys was labeled with the biarsenical compound FlAsH, resulting in 85% labeling efficiency. To determine whether NS3-FlAsH could bind to NS5B, a pull-down experiment was performed. NS5B-coated Dynabeads were used to isolate recombinant NS3, NS3-tetracys, and NS3-FlAsH from solution, whereas NS3 helicase domain was not isolated (Figure 8A). The same gel was examined by fluorescence imaging to illustrate the appearance of NS3-FlAsH (Figure 8B).

On the basis of the finding that NS5B-coated Dynabeads were capable of isolating NS3-FlAsH from solution, fluorescence polarization was utilized to further study the interaction between the two proteins. Three concentrations of NS3-FlAsH were titrated with increasing concentrations

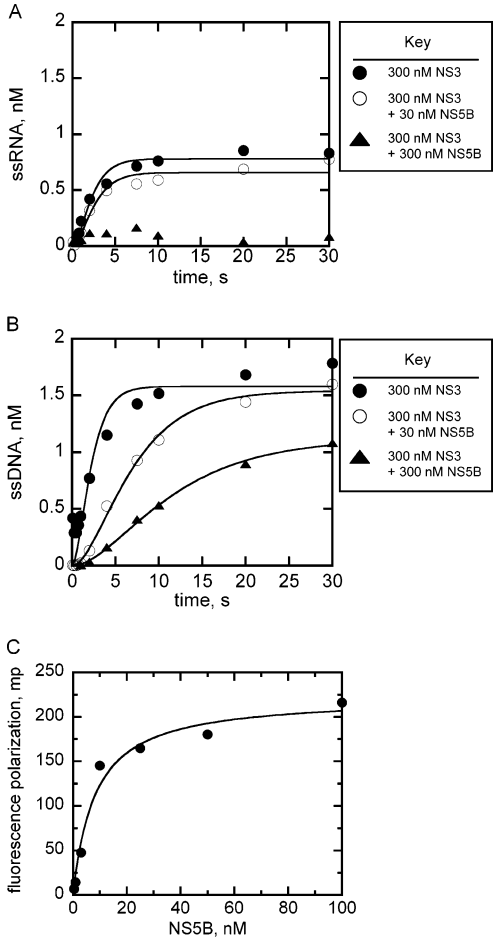


FIGURE 7: NS5B inhibits NS3-catalyzed RNA unwinding when enzyme concentrations are in excess of substrate under single turnover conditions. Unwinding was initiated by mixing 2 nM 60:30mer RNA (panel A) or 2 nM 60:30mer DNA (panel B) with 300 nM NS3 in the absence or presence of various concentrations of NS5B with 5 mM ATP. When NS5B was included, NS3 and NS5B were preincubated 5 min at room temperature before adding the 60:30mer substrate. The unwinding reaction was performed at 37 °C, and the reaction was quenched with 200 mM EDTA + 0.7% SDS. (A) Unwinding of 2 nM 60:30mer RNA was performed by 300 nM NS3 (filled circles) or in the presence of 30 nM NS5B (open circles) or 300 nM NS5B (filled triangles). (B) Identical conditions as above for a 2nM 60:30mer DNA substrate. Curves were fit to a two-step unwinding mechanism, and observed rate constants and amplitudes are shown in Table 1. (C) Binding of NS5B to 15mer DNA as measured by fluorescence polarization. Binding was measured by monitoring changes in fluorescence polarization of a 0.1 nM 5′-fluorescein-labeled 15mer DNA. NS5B binding to F-$(T)_{15}$ resulted in $K_D$ values of 7.7 ± 6.8 nM. Data were fit to the quadratic equation to obtain $K_D$ values using Kaleidagraph (Synergy Software), and standard errors are reported.

of NS5B, and each sample was allowed to incubate for 90 min at 37 °C. The fluorescence polarization decreased at low concentration of NS5B followed by an increase when NS5B was added in excess (Figure 9). The minimum point in the biphasic curve was reached when the concentration of NS5B was the same or similar to the concentration of NS3-FlAsH. This finding indicates that a thermodynamically favorable complex forms between these two proteins with a stoichiometry of ~1:1.

*The Effect of NS5B Unwinding Activity of NS3 under Pre-Steady-State Unwinding Conditions.* Steady conditions may report on association and dissociation of the enzyme from its substrate rather than unwinding, per se. Single turnover

Table 1: RNA and DNA Unwinding by NS3 under Single Turnover Conditions in the Presence or Absence of NS5B[a]

| substrate | NS3 (nM) | NS5B (nM) | observed rate constant ($s^{-1}$) | amplitude (nM) |
|---|---|---|---|---|
| RNA | 300 | - | 0.83 ± 0.09 | 0.78 ± 0.03 nM |
| RNA | 300 | 30 | 0.72 ± 0.09 | 0.66 ± 0.03 nM |
| RNA | 300 | 300 | ND | ND |
| DNA | 300 | - | 0.8 ± 0.2 | 1.6 ± 0.1 nM |
| DNA | 300 | 30 | 0.27 ± 0.01 | 1.54 ± 0.03 nM |
| DNA | 300 | 300 | 0.162 ± 0.005 | 1.11 ± 0.02 nM |

[a] Kinetic parameters were determined from fitting the data in Figure 7 to a two-step mechanism by using the program Kaleidagraph.

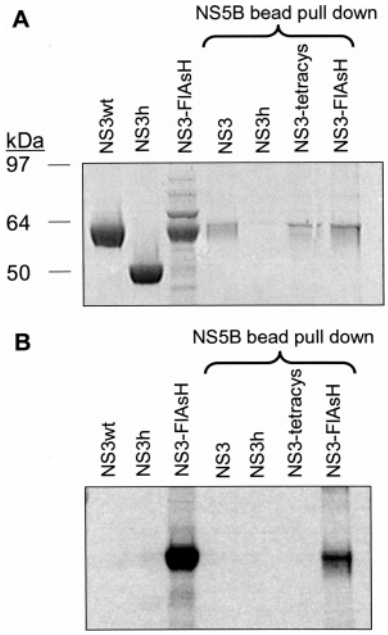


FIGURE 8: NS5B-coated Dynabead pull-down assay with NS3-FlAsH. NS5B-coated beads were incubated with NS3, NS3h, NS3-tetracys, or NS3-FlAsH. Products that bound to the beads were eluted and resolved by 4−20% SDS-PAGE and visualized by (A) Coomassie staining and (B) fluorescent imaging.

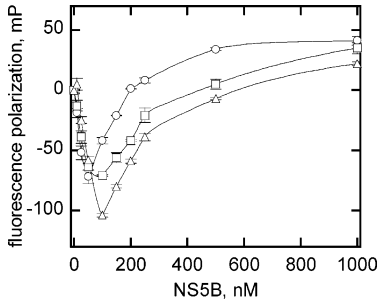


FIGURE 9: Interaction between NS3-FlAsH and NS5B observed by fluorescence polarization. The fluorescence polarization of the following different concentrations of NS3-FlAsH was measured in the presence of increasing concentrations of NS5B: 50 (open circles), 100 (open squares), and 150 nM (open triangles) NS3-FlAsH. Samples were incubated for 90 min at 37 °C. Error bars represent the standard deviation from three independent experiments. Interpolation lines have been added for each curve.

conditions resulted in formation of nonproductive complexes, perhaps due to competition for binding of substrate between NS3 and NS5B. In order to more carefully evaluate the effect of NS5B on the unwinding reaction, experiments were performed under pre-steady-state conditions in which the enzyme and substrate concentrations were similar. Under

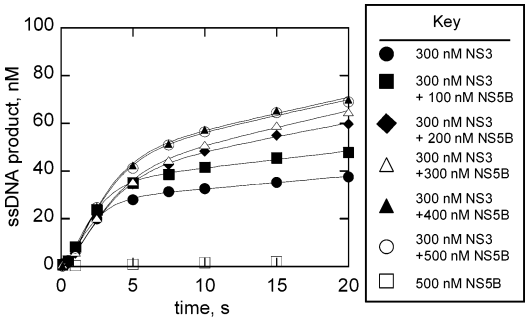


FIGURE 10: Effect of NS5B on unwinding activity of NS3 under pre-steady-state conditions. Unwinding of 100 nM 45:30mer was performed with 300 nM NS3 alone (filled circles) or with 100 nM (closed squares), 200 nM (closed diamonds), 300 nM (open triangles), 400 nM (filled triangles), and 500 nM NS5B (open circles), and with 500 nM NS5B alone (open squares). Proteins were preincubated at 25 °C for 10 min prior to incubation with DNA substrate. Data were fit to a two step unwinding mechanism followed by a steady state, and the observed kinetic parameters are shown in Table 2.

Table 2: DNA Unwinding by NS3 under Pre-Steady-State Conditions in the Presence or Absence of NS5B[a]

| NS5B (nM) | $k_u$ observed ($s^{-1}$) | $k_{ss}$ observed ($nM \cdot s^{-1}$) |
|---|---|---|
| 0 | $0.95 \pm 0.03$ | $0.53 \pm 0.04$ |
| 100 | $0.87 \pm 0.03$ | $0.71 \pm 0.05$ |
| 200 | $0.60 \pm 0.03$ | $1.16 \pm 0.09$ |
| 300 | $0.58 \pm 0.03$ | $1.4 \pm 0.1$ |
| 400 | $0.64 \pm 0.03$ | $1.3 \pm 0.1$ |
| 500 | $0.63 \pm 0.03$ | $1.3 \pm 0.1$ |

[a] Kinetic parameters were determined from fitting the data in Figure 10 to a two step mechanism followed by a steady state using the program Kaleidagraph.

these conditions, the initial unwinding event can be observed as well as multiple cycle events, but the possibility of competitive interactions between the two enzymes for the nucleic acid substrate is minimized.

We have recently optimized conditions for conducting pre-steady-state DNA unwinding with NS3 (Chen et al., in preparation). On the basis of these studies, a 30 bp DNA substrate with a T15 loading strand was selected. The concentrations of NS3 and 45:30mer were held constant at 300 nM and 100 nM, respectively, and the NS5B concentration was varied from 0 to 500 nM (Figure 10). As the concentration of NS5B was increased, product formation was found to increase somewhat until the concentration of NS5B was approximately equal to the concentration of NS3. The steady-state rate increased; however, the observed rate constant for the first phase of unwinding demonstrated a modest reduction as the concentration of NS5B was increased (Table 2). The increase in product formation correlated with a stoichiometry of ~1:1 NS3:NS5B, providing kinetic evidence for a 1:1 complex between these two proteins.

## DISCUSSION

The interaction between polymerase and helicase has become a common view for DNA replication complexes. Von Hippel (*25*) reported functional coupling of the helicase (gp41) and polymerase (gp43) of bacteriophage T4 within the DNA replication fork. The polymerase gp43 can strongly increase the helicase gp41 unwinding activity. The replicative helicase of *Escherichia coli*, DnaB, is also inefficient on its own, but becomes rapid when combined with the chromosomal replicase, DNA polymerase III holoenzyme (Pol III HE) (*46*). Evidence was reported recently that coupling between the bacteriophage T7 helicase and polymerase are coupled such that the polymerase enhances the rate of the helicase (*29*). Investigation of these functional interactions is important for understanding the DNA replication.

In contrast, far fewer studies have explored multiprotein complexes involved in RNA virus replication. Ahlquist reported that the ability of Brome Mosaic Virus 2a polymerase-like protein to interact with 1a helicase-like protein significantly contributes to BMV survival (*47*). Previously Piccininni et al. (*22*) reported that NS3 or NS3h could stimulate the polymerase activity of NS5B and this stimulation is dependent on NS3 ATPase activity. Recently another group reported that NS5B stimulates DNA unwinding activity of NS3. In contrast, a different RNA-dependent RNA polymerase derived from West Nile virus had no effect on NS3 DNA helicase activity (*23*). NS5B is also known to interact with a cellular helicase, p68, and relocalize it from the nucleus to the cytoplasm. When p68 was depleted using specific p68 small interfering RNA, reduction in the transcription of negative-strand from positive-strand HCV RNA was observed (*48*).

The NS3 protease domain appears to mediate interactions with the NS5B polymerase (Figures 1 and 2), consistent with previous reports (*21*, *23*). Data in this report are the first to show that NS5B can stimulate the ssRNA product formation resulting from the unwinding activity of NS3. This is an important new finding since the activity of NS3 has been shown to differ between DNA and RNA substrates (*45*). The functional studies indicate that NS3 may become more efficient in the presence of NS5B because the basal rate of ATPase activity is reduced whereas the RNA helicase activity is enhanced (Figures 4 and 5).

NS5B can stimulate the product formation for RNA unwinding activity of NS3 under multiple turnover conditions in which the nucleic acid substrate concentration is similar to the enzyme concentration. Previous work with DNA substrates demonstrates a similar finding (*23*). Under these conditions, unwinding, per se, is not measured. Steady-state conditions may be more reflective of enzyme association or dissociation with substrate rather than unwinding. To more thoroughly examine unwinding, we carried out experiments under single turnover conditions. These conditions include a vast excess of poly U relative to substrate and enzyme to ensure that enzyme does not have the ability to rebind to fresh substrate after dissociation. Under single turnover conditions, NS5B actually reduces the rate constant for unwinding and the amplitude (Figure 7, Table 1). The same observation is made when a DNA substrate is examined. Investigation under pre-steady-state conditions for DNA unwinding suggests that the interaction between NS3 and NS5B somewhat slows the observed rate constant for unwinding as the concentration of NS5B increases (Figure 10, Table 2). Interestingly, the steady-state rate for product formation was found to increase. A likely explanation for these findings is that NS5B increases the association rate of NS3 with the substrate. Under multiple-cycle reaction conditions, this leads to increased product formation because NS3 associates with substrate more rapidly after dissociation from product. The kinetic results illustrate the importance

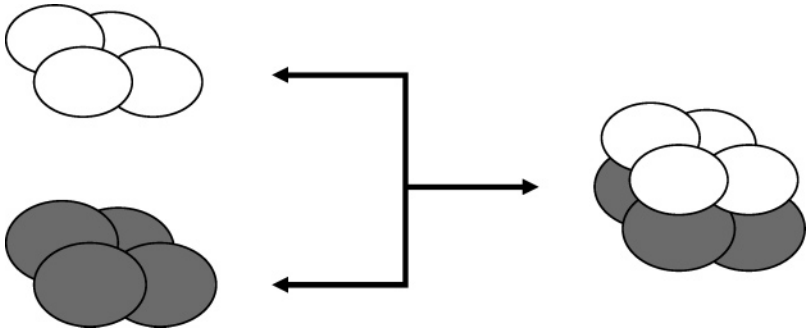

FIGURE 11: Model for interaction between NS3 and NS5B. NS3 (white ovals) and NS5B (gray ovals) independently exist as oligomeric proteins in vitro. A stoichiometric complex forms upon mixing the two proteins.

of conducting pre-steady-state unwinding experiments in order to clearly evaluate the steps that are responsible for increased product formation in multiple turnover experiments. These results illustrate that the interaction between NS3 and NS5B is complex and may involve competition for binding nucleic acids when substrate is limiting. Whether NS5B stimulates or inhibits product formation during NS3-catalyzed nucleic acid unwinding is dependent on the relative concentrations of enzyme and substrate.

The stoichiometry of the NS3−NS5B complex has been difficult to discern owing to the oligomeric nature of each protein *in vitro*. The results from titrating NS3-FlAsH with NS5B provide evidence that a 1:1 complex can form. The reduction in fluorescence polarization might indicate a reduction in the molecular size of the complex, based on the theory of fluorescence polarization (*49*). Alternatively, modeling studies of NS3-tetracys indicate that the tetracysteine cassette is intercalated into the protease domain (Supporting Information Figure 3). As this region is important for the interaction between NS3 and NS5B (Figures 1 and 2, (*21*, *23*), the drop in fluorescence polarization may result from changes in the microenvironment of the fluorescent label. Structural investigations of NS3 have indicated that a great deal of flexibility may exist between the helicase and protease domains (*50*). Binding of NS5B to NS3-FlAsH may result in a global conformational shift such that the fluorescent tag is allowed greater freedom of rotation. An increase in rotation of the fluorophore would account for the observed drop in polarization. The subsequent increase in fluorescence polarization that occurs after addition of excess NS5B may result from formation of a large protein complex, due to NS5B interactions with itself (*39*). Thus, the assay appears to report on the binding of oligomeric NS3 and oligomeric NS5B (Figure 11).

NS3 helicase activity is optimal *in vitro* when the helicase concentration is sufficient to saturate the nucleic acid substrate (*35*, *41*). One explanation for this behavior is that NS3 monomers are not highly processive; therefore, protein−protein interactions help to tether NS3 to the substrate. NS5B could serve a similar role, thereby increasing the processivity of the helicase which would result in greater product formation. These studies provide the first evidence for a 1:1 complex formed between NS5B polymerase and NS3 helicase. The fact that the two proteins are produced as part of a larger poly protein lends support to the notion that a 1:1 complex of these proteins, along with other HCV proteins, may form the core of the HCV replicase.

## ACKNOWLEDGMENT

We thank Lauren Blair for performing molecular modeling studies on NS3 and NS3-tetracys.

## SUPPORTING INFORMATION AVAILABLE

Experimental details. This material is available free of charge via the Internet at http://pubs.acs.org.

## REFERENCES

1. (1997) Hepatitis C: global prevalence, *Wkly. Epidemiol. Rec. 72*, 341−344.
2. Ahmed, A., and Keeffe, E. B. (1999) Overview of interferon therapy for chronic hepatitis C, *Clin Liver Dis. 3*, 757−773.
3. Feld, J. J., and Hoofnagle, J. H. (2005) Mechanism of action of interferon and ribavirin in treatment of hepatitis C, *Nature 436*, 967−972.
4. Lindenbach, B. D., Evans, M. J., Syder, A. J., Wolk, B., Tellinghuisen, T. L., Liu, C. C., Maruyama, T., Hynes, R. O., Burton, D. R., McKeating, J. A., and Rice, C. M. (2005) Complete replication of hepatitis C virus in cell culture, *Science 309*, 623−626.
5. Wakita, T., Pietschmann, T., Kato, T., Date, T., Miyamoto, M., Zhao, Z., Murthy, K., Habermann, A., Krausslich, H. G., Mizokami, M., Bartenschlager, R., and Liang, T. J. (2005) Production of infectious hepatitis C virus in tissue culture from a cloned viral genome, *Nat. Med. 11*, 791−796.
6. Zhong, J., Gastaminza, P., Cheng, G., Kapadia, S., Kato, T., Burton, D. R., Wieland, S. F., Uprichard, S. L., Wakita, T., and Chisari, F. V. (2005) Robust hepatitis C virus infection in vitro, *Proc. Natl. Acad. Sci. U.S.A. 102*, 9294−9299.
7. Reiser, M., Hinrichsen, H., Benhamou, Y., Reesink, H. W., Wedemeyer, H., Avendano, C., Riba, N., Yong, C. L., Nehmiz, G., and Steinmann, G. G. (2005) Antiviral efficacy of NS3-serine protease inhibitor BILN-2061 in patients with chronic genotype 2 and 3 hepatitis C, *Hepatology 41*, 832−835.
8. Sarisky, R. T. (2004) Non-nucleoside inhibitors of the HCV polymerase, *J. Antimicrob. Chemother. 54*, 14−16.
9. Frick, D. N. (2004) The Hepatitis C Virus Replicase: Insights into RNA-dependent RNA Replication and Prospects for Rational Drug Design, *Curr. Org. Chem. 8*, 223−241.
10. Tai, C. L., Chi, W. K., Chen, D. S., and Hwang, L. H. (1996) The helicase activity associated with hepatitis C virus nonstructural protein 3 (NS3), *J. Virol. 70*, 8477−8484.
11. Kim, J. L., Morgenstern, K. A., Griffith, J. P., Dwyer, M. D., Thomson, J. A., Murcko, M. A., Lin, C., and Caron, P. R. (1998) Hepatitis C virus NS3 RNA helicase domain with a bound oligonucleotide: the crystal structure provides insights into the mode of unwinding, *Structure 6*, 89−100.
12. Yan, Y., Li, Y., Munshi, S., Sardana, V., Cole, J. L., Sardana, M., Steinkuehler, C., Tomei, L., De Francesco, R., Kuo, L. C., and Chen, Z. (1998) Complex of NS3 protease and NS4A peptide of BK strain hepatitis C virus: a 2.2 A resolution structure in a hexagonal crystal form, *Protein Sci. 7*, 837−847.
13. Levin, M. K., Gurjar, M., and Patel, S. S. (2005) A Brownian motor mechanism of translocation and strand separation by hepatitis C virus helicase, *Nat. Struct. Mol. Biol. 12*, 429−435.

14. Lesburg, C. A., Cable, M. B., Ferrari, E., Hong, Z., Mannarino, A. F., and Weber, P. C. (1999) Crystal structure of the RNA-dependent RNA polymerase from hepatitis C virus reveals a fully encircled active site, *Nat. Struct. Biol. 6*, 937−943.
15. El Hage, N., and Luo, G. (2003) Replication of hepatitis C virus RNA occurs in a membrane-bound replication complex containing nonstructural viral proteins and RNA, *J. Gen. Virol. 84*, 2761−2769.
16. Gao, L., Aizaki, H., He, J. W., and Lai, M. M. (2004) Interactions between viral nonstructural proteins and host protein hVAP-33 mediate the formation of hepatitis C virus RNA replication complex on lipid raft, *J. Virol. 78*, 3480−3488.
17. Elazar, M., Liu, P., Rice, C. M., and Glenn, J. S. (2004) An N-terminal amphipathic helix in hepatitis C virus (HCV) NS4B mediates membrane association, correct localization of replication complex proteins, and HCV RNA replication, *J. Virol. 78*, 11393−11400.
18. Dimitrova, M., Imbert, I., Kieny, M. P., and Schuster, C. (2003) Protein-protein interactions between hepatitis C virus nonstructural proteins, *J. Virol. 77*, 5401−5414.
19. Quinkert, D., Bartenschlager, R., and Lohmann, V. (2005) Quantitative analysis of the hepatitis C virus replication complex, *J. Virol. 79*, 13594−13605.
20. Egger, D., Wolk, B., Gosert, R., Bianchi, L., Blum, H. E., Moradpour, D., and Bienz, K. (2002) Expression of hepatitis C virus proteins induces distinct membrane alterations including a candidate viral replication complex, *J. Virol. 76*, 5974−5984.
21. Ishido, S., Fujita, T., and Hotta, H. (1998) Complex formation of NS5B with NS3 and NS4A proteins of hepatitis C virus, *Biochem. Biophys. Res Commun. 244*, 35−40.
22. Piccininni, S., Varaklioti, A., Nardelli, M., Dave, B., Raney, K. D., and McCarthy, J. E. (2002) Modulation of the hepatitis C virus RNA-dependent RNA polymerase activity by the non-structural (NS) 3 helicase and the NS4B membrane protein, *J. Biol. Chem. 277*, 45670−45679.
23. Zhang, C., Cai, Z., Kim, Y. C., Kumar, R., Yuan, F., Shi, P. Y., Kao, C., and Luo, G. (2005) Stimulation of hepatitis C virus (HCV) nonstructural protein 3 (NS3) helicase activity by the NS3 protease domain and by HCV RNA-dependent RNA polymerase, *J. Virol. 79*, 8687−8697.
24. Huang, L., Sineva, E. V., Hargittai, M. R., Sharma, S. D., Suthar, M., Raney, K. D., and Cameron, C. E. (2004) Purification and characterization of hepatitis C virus non-structural protein 5A expressed in Escherichia coli, *Protein Expr. Purif. 37*, 144−153.
25. Delagoutte, E., and von Hippel, P. H. (2001) Molecular mechanisms of the functional coupling of the helicase (gp41) and polymerase (gp43) of bacteriophage T4 within the DNA replication fork, *Biochemistry 40*, 4459−4477.
26. Kolodner, R., and Richardson, C. C. (1977) Replication of duplex DNA by bacteriophage T7 DNA polymerase and gene 4 protein is accompanied by hydrolysis of nucleoside 5′-triphosphates, *Proc. Natl. Acad. Sci. U. S. A 74*, 1525−1529.
27. Matson, S. W., Tabor, S., and Richardson, C. C. (1983) The gene 4 protein of bacteriophage T7. Characterization of helicase activity, *J. Biol. Chem. 258*, 14017−14024.
28. Kato, M., Frick, D. N., Lee, J., Tabor, S., Richardson, C. C., and Ellenberger, T. (2001) A complex of the bacteriophage T7 primase-helicase and DNA polymerase directs primer utilization, *J. Biol. Chem. 276*, 21809−21820.
29. Stano, N. M., Jeong, Y. J., Donmez, I., Tummalapalli, P., Levin, M. K., and Patel, S. S. (2005) DNA synthesis provides the driving force to accelerate DNA unwinding by a helicase, *Nature 435*, 370−373.
30. O'Reilly, E. K., Tang, N., Ahlquist, P., and Kao, C. C. (1995) Biochemical and genetic analyses of the interaction between the helicase-like and polymerase-like proteins of the brome mosaic virus, *Virology 214*, 59−71.
31. Morris, P. D., Tackett, A. J., Babb, K., Nanduri, B., Chick, C., Scott, J., and Raney, K. D. (2001) Evidence for a functional monomeric form of the bacteriophage T4 DdA helicase. Dda does not form stable oligomeric structures, *J. Biol. Chem. 276*, 19691−19698.
32. Tackett, A. J., Wei, L., Cameron, C. E., and Raney, K. D. (2001) Unwinding of nucleic acids by HCV NS3 helicase is sensitive to the structure of the duplex, *Nucleic Acids Res. 29*, 565−572.
33. Zhong, W., Ferrari, E., Lesburg, C. A., Maag, D., Ghosh, S. K., Cameron, C. E., Lau, J. Y., and Hong, Z. (2000) Template/primer requirements and single nucleotide incorporation by hepatitis C virus nonstructural protein 5B polymerase, *J. Virol. 74*, 9134−9143.
34. Huang, T. G., and Hackney, D. D. (1994) Drosophila kinesin minimal motor domain expressed in Escherichia coli. Purification and kinetic characterization, *J. Biol. Chem. 269*, 16493−16501.
35. Tackett, A. J., Chen, Y., Cameron, C. E., and Raney, K. D. (2005) Multiple full-length NS3 molecules are required for optimal unwinding of oligonucleotide DNA in vitro, *J. Biol. Chem. 280*, 10797−10806.
36. Amaratunga, M., and Lohman, T. M. (1993) Escherichia coli rep helicase unwinds DNA by an active mechanism, *Biochemistry 32*, 6815−6820.
37. Cramer, J., Jaeger, J., and Restle, T. (2006) Biochemical and pre-steady-state kinetic characterization of the hepatitis C virus RNA polymerase (NS5BDelta21, HC-J4), *Biochemistry 45*, 3610−3619.
38. Qin, W., Luo, H., Nomura, T., Hayashi, N., Yamashita, T., and Murakami, S. (2002) Oligomeric interaction of hepatitis C virus NS5B is critical for catalytic activity of RNA-dependent RNA polymerase, *J. Biol. Chem. 277*, 2132−2137.
39. Wang, Q. M., Hockman, M. A., Staschke, K., Johnson, R. B., Case, K. A., Lu, J., Parsons, S., Zhang, F., Rathnachalam, R., Kirkegaard, K., and Colacino, J. M. (2002) Oligomerization and cooperative RNA synthesis activity of hepatitis C virus RNA-dependent RNA polymerase, *J. Virol. 76*, 3865−3872.
40. Lam, A. M., Rypma, R. S., and Frick, D. N. (2004) Enhanced nucleic acid binding to ATP-bound hepatitis C virus NS3 helicase at low pH activates RNA unwinding, *Nucleic Acids Res. 32*, 4060−4070.
41. Levin, M. K., Wang, Y. H., and Patel, S. S. (2004) The functional interaction of the hepatitis C virus helicase molecules is responsible for unwinding processivity, *J. Biol. Chem. 279*, 26005−26012.
42. Liu, C., Chopra, R., Swanberg, S., Olland, S., O'Connell, J., and Herrmann, S. (2004) Elongation of synthetic RNA templates by hepatitis C virus NS5B polymerase, *J. Biol. Chem. 279*, 10738−10746.
43. Kawaoka, J., Jankowsky, E., and Pyle, A. M. (2004) Backbone tracking by the SF2 helicase NPH-II, *Nat. Struct. Mol. Biol 11*, 526−530.
44. Beran, R. K., Bruno, M. M., Bowers, H. A., Jankowsky, E., and Pyle, A. M. (2006) Robust translocation along a molecular monorail: the NS3 helicase from hepatitis C virus traverses unusually large disruptions in its track, *J. Mol. Biol. 358*, 974−982.
45. Pang, P. S., Jankowsky, E., Planet, P. J., and Pyle, A. M. (2002) The hepatitis C viral NS3 protein is a processive DNA helicase with cofactor enhanced RNA unwinding, *EMBO J. 21*, 1168−1176.
46. Kim, S., Dallmann, H. G., McHenry, C. S., and Marians, K. J. (1996) Coupling of a replicative polymerase and helicase: a tau-DnaB interaction mediates rapid replication fork movement, *Cell 84*, 643−650.
47. Schwartz, M., Chen, J., Janda, M., Sullivan, M., den Boon, J., and Ahlquist, P. (2002) A positive-strand RNA virus replication complex parallels form and function of retrovirus capsids, *Mol. Cell 9*, 505−514.
48. Goh, P. Y., Tan, Y. J., Lim, S. P., Tan, Y. H., Lim, S. G., Fuller-Pace, F., and Hong, W. (2004) Cellular RNA helicase p68 relocalization and interaction with the hepatitis C virus (HCV) NS5B protein and the potential role of p68 in HCV RNA replication, *J. Virol. 78*, 5288−5298.
49. Lundblad, J. R., Laurance, M., and Goodman, R. H. (1996) Fluorescence polarization analysis of protein-DNA and protein-protein interactions, *Mol. Endocrinol. 10*, 607−612.
50. Yao, N., Reichert, P., Taremi, S. S., Prosise, W. W., and Weber, P. C. (1999) Molecular views of viral polyprotein processing revealed by the crystal structure of the hepatitis C virus bifunctional protease-helicase, *Structure 7*, 1353−1363.


BI701048A